Quantitative XANES Analysis of Cuprous Dibromide Complex Formed in the Oxidative Carbonylation of Phenols

Won Bae Kim and Jae Sung Lee*

Department of Chemical Engineering, Pohang University of Science and Technology (POSTECH), San 31, Hyoja-dong, Pohang 790-784, Korea

Received: March 12, 2003; In Final Form: June 29, 2003

Quantitative analysis of Cu K-edge XANES spectra representing mixed states of two cuprous compounds was studied to determine the composition of copper species formed in the oxidative carbonylation of phenols. The quantification of two Cu(I) species, Cu_2O and an unusual cuprous dibromide complex in the linear configuration stabilized with tetrabutylammonium cation, could be achieved through detailed edge analyses to choose proper reference XANES spectra, followed by fitting the experimental XANES spectrum with the linear combination of the two reference spectra. The amount of cuprous dibromide complex obtained by this method showed an excellent correlation with the rate of formation of the desired para-position carbonylation products, indicating that the phase was the active and selective catalytic phase of copper.

Introduction

Oxidative carbonylation of phenol or bisphenol A has been regarded as a promising alternative for synthesis of polycarbonate or its intermediate without employing phosgene.[1−8] Recently, we reported on the nature and role of the active states of catalyst components for the oxidative carbonylation of phenols (OCP) with carbon-supported metallic Pd (Pd/AC), cuprous oxide, and tetrabutylammonium bromide (TBAB or Bu_4NBr).[9] Through characterization by X-ray absorption fine structure (XAFS) of Pd and Cu K-edges for the liquid phase mixture after the OCP reaction, it was concluded that an unusual cuprous dibromide complex was the active main catalyst assisted by the Pd/AC catalyst. Furthermore, particle size variation of metallic Pd on AC did not affect the activity and the selectivity of the desired para-positioned carbonylation products.[10] The cuprous dibromide complex was formed in situ during the OCP reaction by a reaction of Cu_2O with TBAB as depicted below, and its structure was identified by the qualitative X-ray absorption near-edge structure (XANES) of copper.[9]

There are a number of catalytic systems that involve two or more complexes of the same metal component with different geometric structures and electronic states that are formed when an initial metal precursor is converted into other phases during catalytic reactions. The current catalytic system also contained at least two copper states: initially supplied cuprous oxide and the cuprous dibromide complex formed during the reaction.[9] The possibility of other intermediate copper phases was excluded through edge analyses, as will be discussed later. With variation of the relative ratio of TBAB/Cu, the fraction of each copper phase was changed. Furthermore, the reaction rate and the selectivity to the desired para-position carbonylated products also varied markedly. Elucidation of active states for the working catalyst is important, and quantitative analysis for the species involved in the catalytic reaction is of great interest as well.

The purpose of this work is to perform a quantitative analysis for the XANES spectra representing mixed states of two cuprous compounds present in catalysts used for the OCP reaction and to demonstrate its correlation with activity and selectivity. First, a detailed examination of XANES spectra was performed with particular emphasis on the energy and intensity of characteristic peaks in the spectra. From these qualitative analyses we could understand what kinds of species were involved and which would be appropriate reference spectra to be used to fit the experimental XANES spectrum. After these preliminary considerations, we could fit the experimental XANES spectrum by the linear combination of reference XANES spectra to obtain quantitative information about the copper compounds involved in OCP. This method has been successfully applied for quantification of Ti bonding modes such as Ti−O−Si and Ti−O−Ti in Ti−Si binary oxides.[11,12] The results of this quantitative analysis for active catalytic phases were correlated with catalytic activity and selectivity for the OCP reaction, and thus helped us understand the catalytic phenomenon prevailing in our complicated OCP reaction condition.

Experimental Methods

Preparation of Carbon-Supported Pd. Palladium supported on activated carbon (denoted as Pd/AC, 5 wt % Pd) was prepared by a wet impregnation method. Activated carbon (Aldrich, BET surface area of 1075 $m^2\ g^{-1}$), which was dried at 383 K for 12 h in an oven before impregnation, was mixed with a solution of $Pd(CH_3COO)_2$ dissolved in acetone. This slurry was dried at 333 K for 1 h to remove the acetone at atmospheric pressure and dried further under a reduced pressure of ca. 100 Torr in a rotary evaporator. The impregnated catalyst was then reduced into metallic Pd supported on activated carbon with a dihydrogen stream of 37 μmol s^{-1} at 473 K for 4 h in a U-type quartz reactor. The fresh 5 wt % Pd/AC catalyst had a Pd−Pd coordination number of ca. 6.0, as determined by the quantitative EXAFS analyses of Pd K-edge. However, the Pd−Pd coordination number was increased to 11.0 after the OCP reaction, regardless of the amount of TBAB and copper precursor, indicating the particle size of Pd had increased.[9] All reagents except Cu_2O (Alfa) were purchased from Aldrich and were used as received.

* To whom correspondence should be addressed. E-mail: jlee@postech.ac.kr. Phone: 82-54-279-2266. Fax: 82-54-279-5528.

10.1021/jp034627q CCC: $25.00
Published on Web 07/30/2003

SCHEME 1

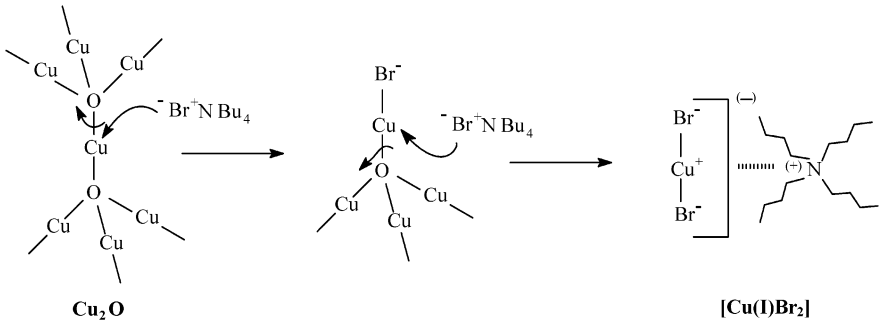

TABLE 1: Sample Designation and Their Reaction Conditions for the Oxidative Carbonylation of Phenols

sample	TBAB/Pd [a] (mol/mol)	Cu_2O/Pd [a] (mol/mol)	TBAB/Cu_2O [b] (mol/mol)
S1	0	10	0.0
S2	5	10	0.5
S3	10	10	1.0
S4	30	10	3.0
S5	50	10	5.0
S6	100	10	10.0
S7	50	1	50.0
	50	3	16.7
S8	50	5	10.0
	50	10	5.0
S9	50	20	2.5
S10	50	50	1.0

[a] All the reaction samples were obtained with the amount of TBAB or Cu_2O relative to a fixed amount of Pd (0.01 mmol). The other reaction variables were the same as mentioned in the Experimental Section. [b] The ratios of TBAB/Cu_2O were calculated from dividing TBAB/Pd by Cu_2O/Pd.

Oxidative Carbonylation of BPA and Phenol (OCP). In a typical reaction, the 5 wt % Pd/AC (0.01 mmol of Pd), 0.1 mmol of Cu_2O, 0.5 mmol of 1,4-benzoquinone (BQ) as an organic cocatalyst, tetrabutylammonium bromide (Bu_4NBr, TBAB) as a base, 30 cm^3 of tetrahydrofuran (THF) as a solvent, 10 mmol of BPA, and 20 mmol of phenol were charged into a 100 cm^3 autoclave (Parr). After the reactor was purged with O_2 three times, 5 MPa of CO and 0.5 MPa of O_2 were charged successively, and the reaction temperature was adjusted to 373 K. The reaction was quenched after 4 h of reaction time by cooling the reactor with ice water. Reaction products were analyzed by high-performance liquid chromatography (HPLC), using the reverse-phase method, gas chromatography (GC), and GC-mass spectrometry (GC/MS) to identify and quantify the polycarbonate precursors as well as byproducts. The reaction procedures were described in detail elsewhere.[8]

For convenience, the reaction mixtures after the OCP reaction were designated by a sample number as described in Table 1. There are two sample series in this work: one with variation of TBAB/Pd ratio and the other with a variation of Cu_2O/Pd. In all cases, the amount of Pd was fixed at 0.01 mmol. Hereafter, all the sample designations will be based on Table 1.

XAS Measurements and Data Analysis. X-ray absorption spectroscopy (XAS) measurements were conducted on beamline 10B of the Photon Factory in the National Laboratory for High Energy Physics (KEK) in Tsukuba, Japan.[13] The spectra were taken at room temperature in a transmission mode for the K-edge of Cu. The X-ray intensity was monitored by using ionization chambers purged with N_2 (100%) for the incident beam and N_2 (85%) + Ar (15%) for the transmitted beam. As standard reference materials, XAS data were obtained for Cu foil, Cu_2O, CuCl, CuBr, CuI, and some cupric compounds such as CuO and $CuBr_2$.

To observe the structure of Cu remaining in the reaction medium and achieve an optimum X-ray transmission intensity, the reaction mixtures containing catalytic components and reagents after the OCP reaction were filtered to reduce the total volume into ca. $^1/_3$ with a 0.45 μm PTFE polymer filter. The filtered catalyst-rich reaction sample was then dried to remove solvent under a reduced pressure, resulting in a gellike mixture of catalytic components and unreacted reagents as well as carbonylation products. This filtration procedure had been introduced in our previous work[9] to increase the X-ray intensity for Pd of Pd/AC catalysts rather than that for Cu since the Pd content was much less than that for Cu (for example, 1/10 of Pd/Cu ratio). This sample preparation method allowed the optimum X-ray absorption for the Cu compounds without disturbing the active state in the reaction medium. Although this preparation procedure was conducted on the condition exposed to atmosphere, there was no possible effect on the resulting Cu phases because the reaction had been carried out already in the presence of dioxygen and water. XAS spectra were obtained with use of a Kapton window-sealed Teflon tubing spacer with an outer diameter of 0.5 in. containing the gellike mixture injected by a syringe just before the measurement. The length of the Teflon tubing spacer was adjusted from 2 to 15 mm according to prior calculations for the optimum X-ray absorption.

The XANES spectra for Cu compounds were analyzed with the WinXAS 97 program.[14] The background correction and the normalization of the spectrum were processed by a least-squares fit. The preedge background was removed by fitting a preedge region with a straight line and by subtracting the extrapolated values from the entire spectrum. The resulting elemental absorption $\mu(E)$ was then normalized by using atomic-like absorption $\mu_0(E)$ at the edge, which was calculated with a cubic spline fit in the postedge region.

XRD Measurements. X-ray diffraction (XRD) measurements were conducted on an X-ray diffractometer (M18XHF, MAC Science Co.), using a radiation source of Cu Kα (λ = 1.5405 Å) at 40 kV and 200 mA with a scanning rate of 4 deg min^{-1}. The samples after the OCP reaction were obtained by the same method as for XAS measurements.

Results

Cu K-edge XANES Spectra of References and Samples. XANES represents electronic transition from an inner level to outer unoccupied levels caused by X-ray absorption, thus giving information on the local electronic state and the coordination environment around an absorbing atom. For this reason, the geometric structure and the oxidation state of copper compounds

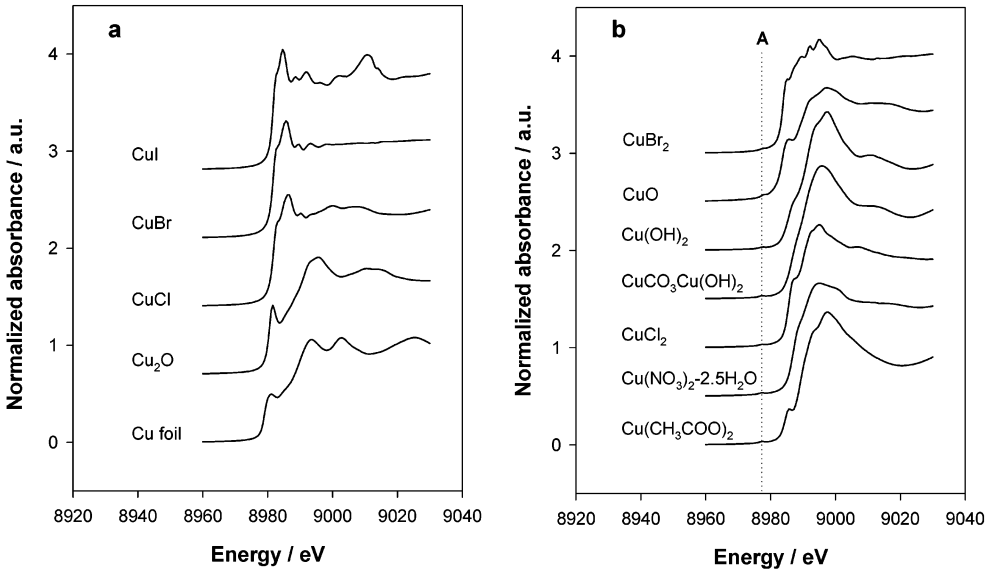

Figure 1. K-edge XANES spectra of reference copper compounds: (a) Cu(0) and Cu(I) compounds, (b) Cu(II) compounds.

have been widely probed by Cu K-edge XANES in qualitative manners such as fingerprinting the shape of spectra and comparing the intensity of characteristic peaks. Figure 1 shows XANES spectra of copper references including some metallic, cuprous, and cupric compounds. The absorption edge of Cu K-edge XANES is assigned to the dipole-allowed 1 s → 4 p transition. While Cu(0) and Cu(I) have no hole in the 3 d orbital, Cu(II) compounds are in a d^9 configuration, thus a weak but characteristic preedge peak representing the quadruple-allowed 1 s → 3 d transition appears below the edge in most Cu(II) compounds. This characteristic preedge peak observed in most cupric compounds was denoted as "peak A" and located at the vertical dashed line in Figure 1b. Its presence could be unambiguously determined from the 1st and 2nd derivatives of the XANES spectrum. Therefore, the presence of peak A could be regarded as a signature for a divalent copper together with a higher edge energy E_0 compared to those of Cu(0) and Cu(I) compounds. The edge position for the Cu references is defined as the maximum point of the 1st derivative function in the rapidly rising edge step of the absorbance vs energy plot. Its values were determined to be 8979.0, 8980.6, 8981.6, 8983.6, and 8983.8 eV for Cu foil, Cu_2O, CuBr, CuO, and $CuBr_2$, respectively, representing the expected trend, i.e., increased edge energies as the oxidation number is raised.

We investigated the Cu K-edge XANES spectra of the used catalysts contained in the samples S1−S10, as illustrated in Figure 2. These samples were obtained by varying the ratios of TBAB/Pd and Cu_2O/Pd, and these variations would naturally change the ratio of TBAB/Cu_2O, as indicated in Table 1. The spectra showed systematic changes of the entire XANES shape as well as peak intensity at 8980−8985 eV. The peak intensity increased from S1 to S6 or S7, followed by a decrease after S7. For S1 and S10, the entire XANES shape looked like the shape for Cu_2O. The peak at 8980−8985 eV was assigned as "peak B" whose characteristics were investigated and discussed in our previous work[9] in relation to the structure of a new Cu phase present in the samples S4−S6. Briefly, all the samples contained monovalent Cu species, as evidenced by the edge energies and the absence of the preedge peak A corresponding to the 1 s → 3 d transition. XANES spectra for S6 and S7 were typical for the cuprous dibromide complex, [Cu(I)Br_2], as described in Scheme 1. Therefore, the evolution of XANES in Figure 2 implied the structural transformation of Cu from Cu_2O

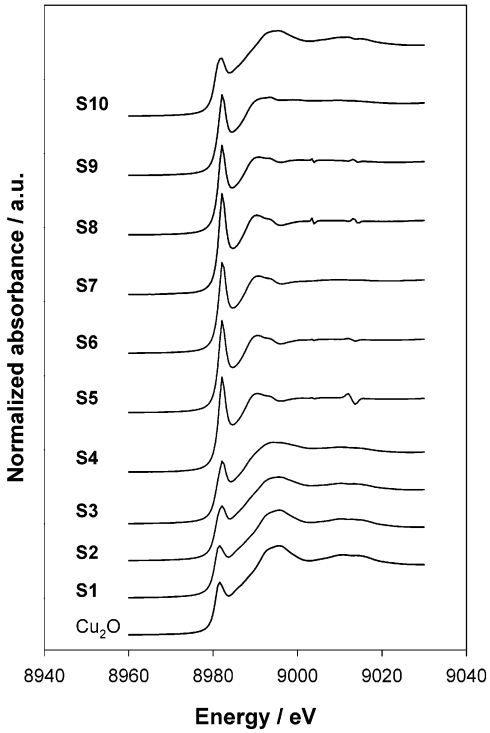

Figure 2. Cu K-edge XANES spectra of the samples S1−S10 after the oxidative carbonylation of phenols at 373 K.

into [Cu(I)Br_2] as the TBAB/Cu_2O ratio increased, suggesting that the formation of the [Cu(I)Br_2] complex depended on the relative ratio of TBAB to Cu_2O. The role of TBAB appeared to be to stabilize the cuprous dibromide complex by forming the structure shown in Scheme 1. This kind of Cu(I) complex was also reported by Rothe et al.,[15] who observed a monovalent Cu in a linear 2-fold coordination with Br anions as an intermediate structure during the preparation of N(octyl)$_4$-stabilized metallic Cu colloid through reducing the [N(octyl)$_4$]$_2$-[$CuCl_2Br_2$] complex by Li[BEt_3H] in toluene. Their XANES spectrum of the monovalent Cu in the linear 2-fold coordination with Br anions was very similar to our XANES spectrum for S7 in terms of the normalized intensity and the calibrated energy position of peak B, as well as the shape of the entire XANES spectrum.

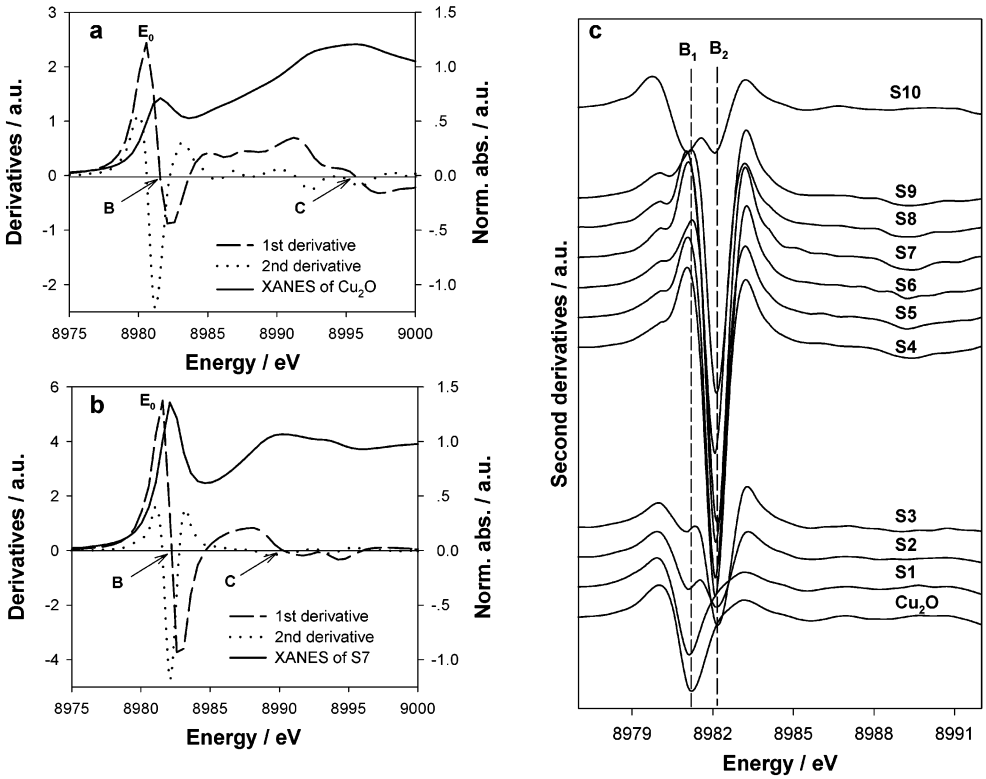

Figure 3. E_0 determination and peak assignments through the 1st and 2nd derivatives of Cu K-edge XANES for the Cu_2O and the sample S7 (a, b) and the changes of the 2nd derivative functions (c).

Detailed Edge Analyses for Cu(I) K-edge XANES Spectra. Figure 3a,b shows the derivative functions of XANES spectra for Cu_2O and S7. The edge energy, E_0, is defined as the energy position corresponding to the peak maximum of the 1st derivative function. For cuprous compounds, peaks B and C correspond to the degenerate 1 s $\rightarrow$ 4 $p_{x,y}$ transition and 1 s $\rightarrow$ 4 p_z transition, respectively, according to ligand field splitting of Cu 4 p orbitals.[16−18] Thus, a linear Cu(I) with two coordinated ligands would involve a repulsive interaction along the *z* axis, raising the energy of the antibonding copper 4 p_z molecular orbitals relative to the 4 $p_{x,y}$ levels. In addition, covalent ligand overlap along the *z* axis will reduce the intensity of the 1 s $\rightarrow$ 4 p_z transition, as this mixing lowers the Cu 4 p_z character in this antibonding orbital. Therefore, the transition from 1 s to the doubly degenerate 4 $p_{x,y}$ final state would result in an intense peak at a lower energy than for the 1 s $\rightarrow$ 4 p_z transition.[16]

Compared with the XANES of Cu_2O, the XANES spectrum of S7 reveals slightly higher energy positions by ca. 1 eV for both the edge energy E_0 and peak B, but shows a lower energy position for peak C by ca. 5 eV. These characteristic differences in the locations of peaks B and C as well as the edge energy enable us to differentiate Cu(I) K-edge XANES spectra prior to the quantification in the next section. More importantly, as shown in Figure 3c, peak B shows two local minima in the second derivative functions for some samples such as S2, S3, and S10. Cu_2O has a single peak assigned as peak B_1, and sample S1 shows the same shape. However, S2 and S3 reveal another peak denoted as peak B_2. Thus peak B in those samples consists of two subpeaks: one from Cu_2O and the other from a new species present in S4−S9. The stronger intensity of peak B_2 seems to overwhelm the relatively weak B_1 for S4−S9, therefore only a single peak appears for these samples even though some of them might contain peak B_1 as well. S10 shows two peaks again because it contains Cu_2O as the main component, as evidenced from the overall shape of the XANES spectrum in Figure 2. The existence of two subpeaks for peak B in some samples implies that samples S1−S10 should involve the two-site model consisting of Cu_2O and the species represented by S7. There was no evidence for any other intermediate phases of copper that might have been involved in the transformation of Cu_2O into [Cu(I)Br_2]. Therefore, the states of Cu in the samples could be represented by the linear combination of the two cuprous compounds.

Figures 4 and 5 show results of detailed analyses of the XANES features, with emphasis on the energy position and intensity of peaks B and C. The edge energy for samples S1−S10 varied within a low limit, corresponding to Cu_2O, and a high limit, corresponding to the CuBr reference. The E_0 shows a maximum around S7. The peak B energy shows a similar trend to that of E_0, but the position of peak C reveals the opposite tendency, showing a minimum around S7. Figure 5 shows a change of peak B intensity in terms of peak heights and peak areas. The areas were obtained by integration of the XANES spectra between −3 and +2 eV around the energy position where peak B showed the maximum height. The peak B area increased up to sample S7 and then decreased afterward. The maximum peak B area at S7 indicates that the copper in the sample is in the cuprous dibromide form with the highest purity. Also the energy positions of E_0, peak B and peak C in Figure 4, support the consistent picture that sample S7 has the highest purity of the [Cu(I)Br_2] species among samples S1−S10.

For Cu(I) complexes, the energy, shape, and intensity of peak B correlates with the nature of ligands and the site geometry of the cuprous ions. The intensity of the peak increases as the coordination number of the Cu(I) ligand decreases from 4 to 2 or the coordination symmetry decreases.[16,17] Thus, a very intense and narrow peak B indicates that the Cu(I) structure is two-coordinated and linear.[15−18] Intensities of peak B for our S5−S8 samples were compared against a plot of normalized peak intensity vs energy based on measurements for 19 Cu(I) and

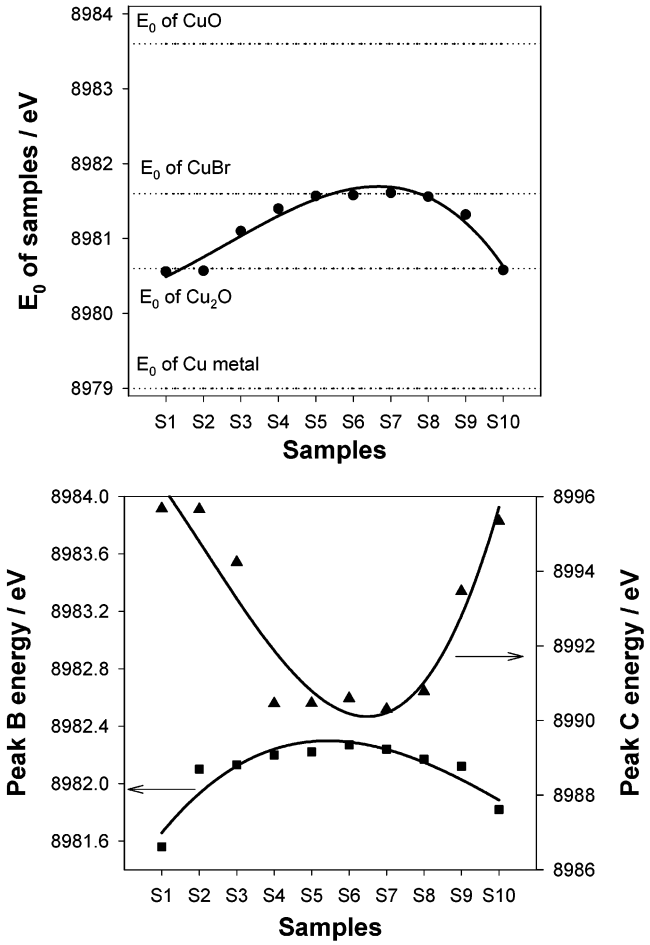

Figure 4. Energy positions of E_0, peak B and peak C, in the Cu K-edge XANES for the samples S1−S10.

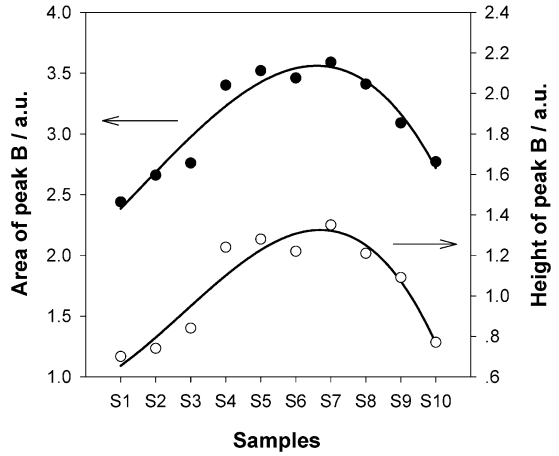

Figure 5. Areas and heights of peak B in the Cu K-edge XANES for the samples S1−S10.

40 Cu(II) model complexes compiled by Kau et al.[16] The values for reference sample S7 fell on the region of Cu(I) with coordination number 2, even with a slightly higher intensity than the values on the plot. This result indicates again the fact that our $Cu(I)Br_2$ complex in sample S7 was pure with linear geometry.

XANES Fitting by the Linear Combination Model of Two Cu(I) Compounds. Considerations in previous sections indicate that a quantitative analysis of our samples could be possible by the linear combination of XANES spectra of Cu_2O and [Cu(I)Br_2]. According to our experience in other systems,[11,12] the selection of proper references is the most important factor for this quantification method to give a reliable and successful result.[12] One natural reference is authentic Cu_2O. The other is S7, which contains the maximum amount of [Cu(I)Br_2] species without any indication of cuprous oxide or other intermediates. Furthermore, this linear-combination model can be justified because the two basis functions employed as reference spectra do not interact with each other. The [Cu(I)Br_2] and Cu_2O have not only different XANES shapes, but also different positions and intensities of the characteristic peaks B and C.

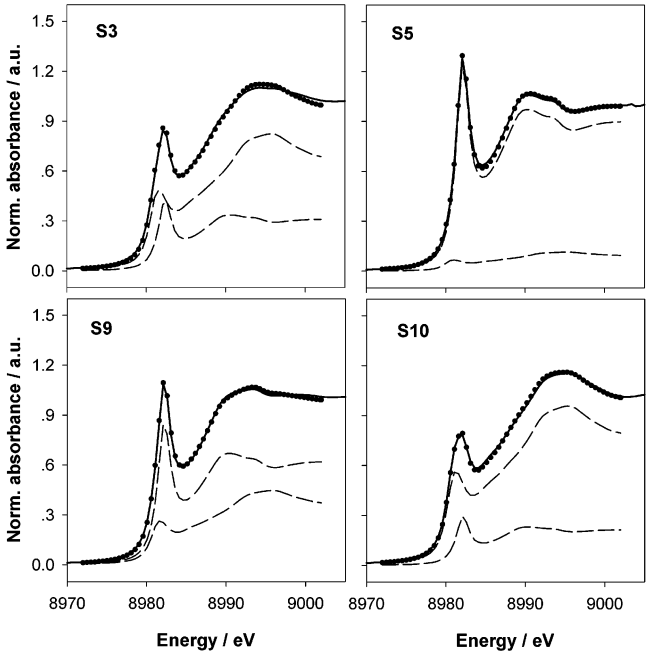

Figure 6. Examples of Cu K-edge XANES fittings for the experimental XANES spectra by the linear combination of reference XANES spectra of Cu_2O and [Cu(I)Br_2]. The solid line is the experimental XANES spectrum and the black dotted is the fitted function. Deconvoluted reference spectra were also included as dashed lines.

The XANES fitting by the linear combination was carried out with two reference XANES spectra of Cu_2O and [Cu(I)-Br_2] (S7) to quantify the fractions of these Cu(I) compounds in the samples S1−S10. Figure 6 demonstrates some examples of the fitting procedure, and their fitting results are listed in Table 2. The fitting range should be chosen to cover both characteristic peaks B and C. There are four parameters to be fitted with two references: two are partial concentrations of Cu_2O and [Cu(I)-Br_2] and the others are energy shift corrections for each reference XANES spectrum, though the latter are not listed in Table 2. Their values were all less than 2%. A parameter related to the quality of the fit, the residual (r), is defined in a footnote to the table. We introduced another term "SOPC" to check the validity of the quantification procedure as well as the choice of references. SOPC refers to "summation of the partial concentration" of Cu_2O and [Cu(I)Br_2] before normalization. This value should be unity if each step of the quantification procedure is correct, including the choice of the reference materials in the XANES fitting.[12]

The SOPC values were all close to unity in the range of 1.00 $\pm$ 0.02, as expected for a valid analysis with "good" references. The best-simulated fitting functions exactly matched the experimental XANES spectra as shown in Figure 6. The calculated fractions of Cu_2O and [Cu(I)Br_2] were listed in Table 2 for samples S1−S10. The fraction of Cu_2O decreased up to S7, which consisted of hypothetically pure [Cu(I)Br_2] without any Cu_2O, and increased above sample S7. The marked decrease in

TABLE 2: XANES Fitting Parameters and Error Analysis for Cu K-edge Obtained from the Fitting Procedure by the Linear Combination of XANES Spectra

	fraction of Cu				
sample	in $Cu(I)Br_2$[a]	in Cu_2O[a]	r[b]	σ[c] ($\times 10^{-3}$)	SOPC[d]
S1	0.030	0.970	1.52	1.00	1.002
S2	0.186	0.814	2.01	1.00	0.995
S3	0.316	0.684	1.87	1.00	0.997
S4	0.897	0.103	1.11	8.70	0.982
S5	0.906	0.094	1.06	6.28	1.006
S6	0.892	0.108	0.66	6.53	0.985
S8	0.809	0.191	1.49	3.29	1.007
S9	0.630	0.370	1.29	4.09	0.999
S10	0.215	0.785	1.16	1.00	1.009

[a] Normalized Cu concentration (±0.03 at maximum, mole fraction). [b] Residual (%) is the sum of fractional misfit, which is defined as

$$r = 100\sum_{i=1}^{N}|y_{exp}(i) - y_{theo}(i)|/\sum_{i=1}^{N}|y_{exp}(i)|$$

where N is the number of data points, σ is an estimate for the experimental error, and y_{exp} and y_{theo} are experimental and fitted values, respectively. [c] Experimental error generated from the WinXAS program. [d] Sum of partial concentrations before normalization.

the Cu_2O fraction at S3−S4 and the large increase at S8−S10 are accompanied by simultaneous great changes in the fraction of $[Cu(I)Br_2]$ in the opposite direction as shown in the table.

Discussion

XANES studies have been performed in many fields of materials and catalysts characterization due to the sensitivity to local coordination geometry and electronic structure around the X-ray absorbing metal of interest. There have been many attempts to quantitatively analyze the copper K-edge XANES, which contains rich fine features representing electronic structure and coordination environment.[19] The Cu K-edge XANES of a calcined Cu−ZnO methanol synthesis catalyst was subtracted by a reference spectrum to obtain the relative amount of cupric oxide and a Cu(II) species doped into the tetrahedral sites of the ZnO lattice.[20] Liu and Robota[21] studied the oxidation state and coordination environment of a Cu-exchanged ZSM-5 catalyst for selective catalytic reduction of NO by hydrocarbon. They also utilized the difference between Cu K-edge XANES of the sample containing Cu(I) species and that of metallic Cu over a narrow energy window of 10 eV, which represented the characteristic 1 s to 4 p transition of the Cu(I) species. Kumashiro et al.[22] investigated quantification of Cu(I) species of Cu-exchanged ZSM-5 catalyst during heat treatment through selection of an adequate reference for Cu(I) and then estimation of the amount of the Cu(I) species by comparing an experimental XANES spectrum with reference spectra calculated with appropriate weighting factors. It could be an improved technique in quantification, compared to previous methods such as the interpretation via intensity comparison of a particular peak or difference between XANES spectra, since this method enables one to fit the entire XANES spectrum with reference spectra and to see the extent of matching. For practical applications of the quantitative XANES analysis to catalytic systems involving copper, a mathematical procedure has been established based on factor analysis[23−25] or principal component analysis.[26,27] The methodological procedure involves the proper selection of factors or principal components which comprise an experimental Cu K-edge XANES spectrum in a mathematical manner to determine the number and the type of involved Cu species. Each contribution to the XANES spectrum then can be obtained as concentration through fitting the experimental spectrum with the linear combination of the simulated reference spectra called factors or principal components. These fitting procedures have been adopted successfully with good agreement in the following studies: quantification of Cu(I) and Cu(II) species over CuZSM-5,[23] quantitative analysis of a reduced and an oxidized Cu and a mixed Cu−Pd oxide over CuPd/zeolite,[24] concentration profiles of Cu(0), Cu(I), and Cu(II) in temperature-programmed reduction of CuZSM-5 catalysts,[26] and Cu metal and CuO over Cu/SiO_2 catalyst in a specific reducing atmosphere.[27]

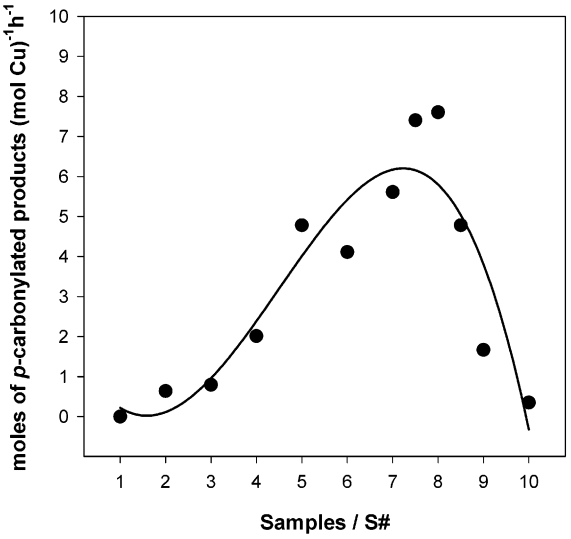

Figure 7. Activity of the oxidative carbonylation of phenols over the samples S1−S10.

For the quantitative analyses, however, the selection of proper references is one of the most difficult and important parts in obtaining correct composition, when there is no universal reference that can represent the experimental spectra. As we observed the unusual cuprous dibromide complex that was formed in situ during the OCP reaction, it was required to confirm the nature of the Cu species and its purity prior to performing the quantitative analysis by the linear combination of reference XANES spectra. A reliable and convenient method for the quantification of Cu(I) compounds was utilized here from the detailed Cu K-edge analysis, followed by the linear combination (LC) of experimental reference XANES spectra, which had been successfully applied to Ti−Si binary oxides.[11,12] Through the detailed edge analysis, Cu_2O was chosen as one reference of the Cu(I) compound because our system contained only two compounds of Cu_2O and $[Cu(I)Br_2]$. To find a proper reference XANES spectrum for $[Cu(I)Br_2]$, careful considerations were made. The characteristics of the Cu K-edge XANES spectra for Cu_2O and the samples S1−S10 used were investigated in detail. Attention was focused on the changes in the intensity and the energy position of the characteristic peak B. The sample S7 showed the highest peak B intensity with the maximum area. Furthermore, the energy positions of E_0 and peak B showed the highest values around S7. Therefore, the Cu(I) complex (i.e. $[Cu(I)Br_2][NBu_4]$) should exist in the sample S7 with the highest purity in the absence of any indication of the cuprous oxide phase.

There existed two kinds of Cu(I) structures in the present reaction system of OCP. The fractions of Cu_2O and $[Cu(I)Br_2]$ were directly related to the ratio of TBAB to Cu_2O. The $[Cu(I)Br_2]$ species produced from Cu_2O by TBAB played an important role in the activity and selectivity in the OCP reaction.[9] Figure 7 shows the reaction rates calculated from the BPA conversions divided by the total number of Cu introduced in the reaction system. The rates increased from S1, showing a maximum value around S7, then decreased rapidly toward the value for S10. It is interesting to note how the Cu-based rate

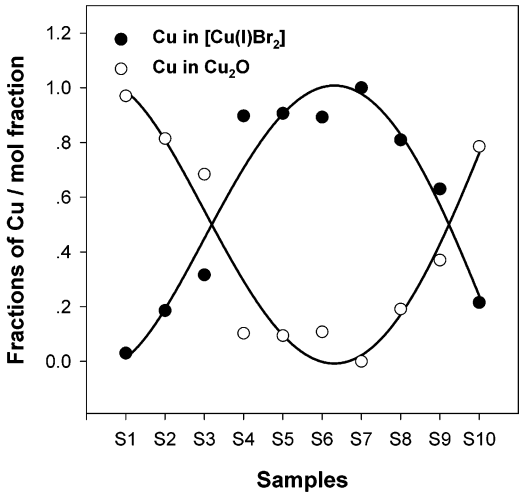

Figure 8. Fractions of Cu in Cu_2O and $[Cu(I)Br_2]$ obtained from Cu K-edge XANES fittings for the samples S1−S10.

profile correlates with the fraction of copper phases obtained by the linear combination of two reference XANES spectra. Figure 8 shows the fractions of two cuprous compounds for all the samples. Compared with Figure 7, we can observe a remarkable correspondence between the rate of formation of para-positioned carbonylation products and the amount of $[Cu(I)Br_2]$. The amount of Cu_2O had no effect at all. Therefore, it is quite clear that the $[Cu(I)Br_2]$ phase must be an active and selective catalyst for the OCP under our reaction condition. This quantitative correlation of the reaction rate with the copper structure provides additional evidence that supports our previous suggestion on the active catalytic phase of the OCP reaction in the presence of Pd/AC, Cu_2O, and TBAB. Thus, Cu_2O was transformed into the $[Cu(I)Br_2]^{-}$- -$^{+}NBu_4$ complex by TBAB during the reaction and this cuprous complex was the active catalyst.[9] The structure of the complex was determined by Cu K-edge XANES and EXAFS.

The samples were also analyzed by X-ray diffraction (XRD). The marked decrease in the fraction of Cu_2O at S3−S4 and the significant increase at S8−S10 in Figure 8 are accompanied by important changes in their XRD patterns as shown in Figure 9: the appearance of sharp diffraction peaks in S2, S9, and S10 due to Cu_2O. There were no XRD peaks of the $[Cu(I)Br_2]$ species since it should be present as an isolated species dissolved completely in the reaction media.

The quantitative XANES analysis employed in this work looks for the suitable reference XANES spectrum among the series of samples prepared with the variation of their phase purity. This method could have a few advantages for quantifying mixed states of a metal component. It allows the quantitative analysis with XANES spectra to be simple and precise because it uses the least number of reference spectra selected from detailed edge analysis of experimental XANES without any possible involvement of meaningless references. Moreover, it could remove a possible effect on XANES spectra caused by differences in the degree of structural disorder, which may be present between the samples to be analyzed and the selected references. This effect has been known to give a significant effect on XANES.[28] However, adopted references in this method are expected to have a similar extent of structural disorder to the samples since we obtain that series of samples under the same preparation conditions. Of course, detailed analysis of XANES spectra and sufficient understanding of the chemical nature of the samples are required in the selection of suitable references. Finally, the validity of this whole procedure could be collectively checked by the SOPC term. In any case, this work could be one of the rare examples in catalysis where a strong case has been made to identify catalytic activity with an explicit site in a complex reaction mixture.

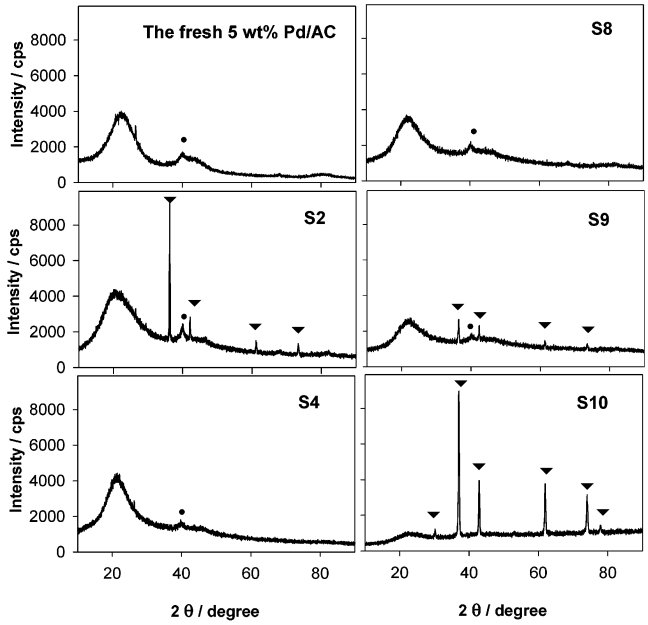

Figure 9. X-ray diffraction patterns of the fresh 5 wt % Pd/AC and some representative samples: Pd metal phase (●) and Cu_2O phase (▼).

Conclusions

Quantitative analysis of Cu(I) compounds formed in the oxidative carbonylation of phenols was made through XANES fitting by the linear combination of two reference spectra. The justification of the two-site model utilized in this work and the selection procedure of proper references were thoroughly considered for the experimental XANES spectra through the detailed edge analyses. The formation and amount of the active cuprous dibromide complex depended on the relative ratio of tetrabutylammonium bromide to cuprous oxide initially introduced into the reaction system. The cuprous dibromide complex was confirmed to be the active catalyst for the oxidative carbonylation of phenols since its amount showed an excellent correlation with the reaction rate based on the moles of desired para-position carbonylation products per mole of copper introduced.

Acknowledgment. This work was supported by KOSEF through the Research Center for Energy Conversion and Storage, the National Nanotechnogy program, and the BK 21 program.

References and Notes

(1) Hallgren, J. E.; Lucas, G. M.; Mathews, R. O. *J. Organomet. Chem.* **1981**, *204*, 135.
(2) Vavasori, A.; Toniolo, L. *J. Mol. Catal. A* **1999**, *139*, 109.
(3) Ishii, H.; Goyal, M.; Ueda, M.; Takeuchi, K.; Asai, M. *Appl. Catal. A* **2000**, *201*, 101.
(4) Takagi, M.; Miyagi, H.; Yoneyama, T.; Ohgomori, Y. *J. Mol. Catal. A* **1998**, *129*, L1.
(5) Song, H. Y.; Park, E. D.; Lee, J. S. *J. Mol. Catal. A* **2000**, *154*, 243.
(6) Goyal, M.; Nagahata, R.; Sugiyama, J.; Asai, M.; Ueda, M.; Takeuchi, K. *Polymer* **2000**, *41*, 2289.
(7) Chaudhari, R. V.; Kelkar, A. A.; Gupte, S. P.; Ghanage, B. M.; Qureshi, M. S.; Moasser, B.; Pressman, E. J.; Sivaram, S.; Avadhari, C. V.; Kanagasabapathy, S. US Patent 6,222,002, 2001.
(8) Kim, W. B.; Park, K. H.; Lee, J. S. *J. Mol. Catal. A* **2002**, *184*, 39.
(9) Kim, W. B.; Park, E. D.; Lee, C. W.; Lee, J. S. *J. Catal.* **2003**, *218*, 334.

(10) Kim, W. B.; Park, E. D.; Lee, J. S. *Appl. Catal. A* **2003**, *242*, 335.
(11) Kim, W. B.; Choi, S. H.; Lee, J. S. *J. Phys. Chem. B* **2000**, *104*, 8670.
(12) Lee, J. S.; Kim, W. B.; Choi, S. H. *J. Synchrotron Radiat.* **2001**, *8*, 163.
(13) Nomura, M.; Koyama, A. *KEK Rep.* **1989**, *89*, 16.
(14) Ressler, T. *J. Phys. IV* **1997**, *7*, 269.
(15) Rothe, J.; Hormes, J.; Bönnemann, H.; Brijoux W.; Siepen, K. *J. Am. Chem. Soc.* **1998**, *120*, 6019.
(16) Kau, L.-S.; Spira-Solomon, D. J.; Penner-Hahn, J. E.; Hodgson, K. O.; Solomon, E. I. *J. Am. Chem. Soc.* **1987**, *109*, 6433.
(17) Moen, A.; Nicholson, D. G.; Rønnig, M. *J. Chem. Soc., Faraday Trans.* **1995**, *91*, 3189.
(18) Lamble, G.; Moen A.; Nicholson, G. *J. Chem. Soc., Faraday Trans.* **1994**, *90*, 2211.
(19) F.-García, M. *Catal. Rev. Sci. Eng.* **2002**, *44*, 59.
(20) Kau, L.-S.; Hodgson, K. O.; Solomon, E. I. *J. Am. Chem. Soc.* **1989**, *111*, 7103.
(21) Liu, D.-J.; Robota, H. J. *J. Phys. Chem. B* **1999**, *103*, 2755.
(22) Kumashiro, R.; Kuroda Y.; Nagao, M. *J. Phys. Chem. B* **1999**, *103*, 89.
(23) Marquez-Alvarez, C.; Rodriguez-Ramos, I.; Guerrero-Ruiz, A.; Haller, G. L.; Fernandez-García, M. *J. Am. Chem. Soc.* **1997**, *119*, 2905.
(24) Fernandez-García, M.; Alvarez, C. M.; Haller, G. L. *J. Phys. Chem.* **1995**, *99*, 12565.
(25) Fernandez-García, M.; Haller, G. L. *J. Phys. IV* **1997**, *7*, 895.
(26) Costa, P. D.; Modén, B.; Meitzner, G. D.; Lee, D. K.; Iglesia, E. *Phys. Chem. Chem. Phys.* **2002**, *4*, 4590.
(27) Meitzner, G. D.; Iglesia, E. *Catal. Today* **1999**, *53*, 433.
(28) Farges, F.; Brown, G. E.; Rehr, J. J., *Phys. Rev. B* **1997**, *56*, 1809